Development of empirical relations to compute the heat transfer coefficients for distiller operating in different operating modes

M.K. Gaur[a,*], G.N. Tiwari[b], Pushpendra Singh[a], Anand Kushwah[a]

[a]Department of Mechanical Engineering, Madhav Institute of Technology & Science, Gwalior 474005, India, Tel. +91 9425020318;
email: gmanojkumar@rediffmail.com (M.K. Gaur), Tel. +91 8878232280; email: pushpendra852@gmail.com (P. Singh),
Tel. +91 7999671338; email: anand.kushwah1989@gmail.com (A. Kushwah)
[b]Research and Development Cell, SRM University, Lucknow, Uttar Pradesh 225003, India, Tel. +9968344488;
email: gntiwari@ces.iitd.ernet.in

a b s t r a c t

The paper focuses on the performance assessment and development of mathematical expressions for calculating heat and mass transfer coefficients for a distiller operating in two modes: (i) condensing cover cooled with ice and (ii) condensing cover without cooled. These expressions are simulated for interior and exterior condition for different water temperature ranging between 35°C and 85°C. Empirical relations are developed for finding the condensing cover temperature at a certain water temperature. The value calculated from the derived empirical relations is used for finding the values of heat transfer coefficients and yield. Result shows that predicted and numerical value are nearly same (less than 2% difference). The predicted value of yield deviates maximum of 3% from numerical and 5.7% from experimental value.

Keywords: Indoor distillation; Empirical relations; Cover temperature; Distillate yield

1. Introduction

Nowadays, the scarcity of pure water is getting worse around the globe and several regions of India are already evident of this. Human activities are merely responsible for fresh water crisis. The areas of water shortage have been expanded due to population growth, improvement of life style and an unusual transformation of the global climate since 1960.

Distillation is a very old technique of making water drinkable from saline/brackish water in far-flung areas. Aristotle in fourth century BC described this process of making brackish water pure through evaporation and condensation. Solar distillation may prove as a best alternative due to its sustainable and eco-friendly operation.

The demand of saline seawater purification and its applications has been increased in recent years. Enormous study had taken place on design, fabrication methods, testing and performance evaluation, etc. of solar distillations around the globe to increase their yield and efficiency. The distillation systems are broadly classified as passive [1–6] and active [7–9] distillation system. Solar energy is first utilized for desalination of seawater. The systematic effort for making the saline water pure was started six decades ago [10].

To increase the yield of still, the temperature difference between feed water and condensing cover must be increased. This can be done either by supplying water at high temperature or by cooling condensing cover or both. Preheating the supply water by using an artificial heat supply is also a method of enhancing the yield of solar stills [11].

* Corresponding author.

For different design considerations of solar still, digital computer was used to find the solution of various heat and mass transfer equations [12]. Morse and Read [13] have analyzed the thermal capability of the proposed system in transient and also expressed that heat flux is dependent on temperature of glass. They determined the cover temperature by using graphical solutions.

Various researches are carried out on condensing cover cooled by water film flowing above it [14–16]. Phadatare and Verma [17] have examined the consequence of cover materials on heat and mass transfer coefficients of plastic solar still. They have observed that the glass covered plastic solar still produces 30%–35% more output than the Plexiglass covered plastic solar still. Yousef and Mousa [18] carried out thermal modeling of a regenerative type solar desalination and reported 20% higher yield than conventional solar still. Thermal analysis is done by Singh and Tiwari [19] for various alignments of a passive regenerative solar still and validates the outcomes with reasonable agreement.

The day time production of solar still can be supplemented by nocturnal production. During day time, the solar energy is available for heating brackish/saline water but during night waste heat from various thermal power plants can be utilized into the distillers. The latest work on night-time working of the solar still [20–24] was described by Grune et al. [20]. They observed that the warm water increases the daily yield of the solar still by two times. For predicting the temperature of glass cover, semi empirical expressions have been developed by Sharma and Mullick [25] for solar still operating on passive mode. Various researchers like Kumar and Sinha [26], Sartori [27] etc. have developed the energy balance equations with some new approach on active and passive solar still operating on different modes. They validated their speculative results with the experimental data.

The paper presents the simplified empirical relations developed to find the heat and mass transfer coefficients in two operating mode of distiller (i.e., with ice cooled and without cooled cover) based on the indoor simulation at IIT Delhi, India. The expressions are used to find the cover temperature at particular temperature of water, which is further used to find the hourly distillate yield. The equations developed are in simplified form than the approximate (numerical) solution. The predicted result obtained is compared with obtained result using numerical solution for the distiller operating at nearly freezing temperature (specific to cold areas) and also at normal temperature of condensing cover. This research can be applied in general for distillers operating in cold countries, where the night temperature reaches nearly to the freezing temperature.

2. Experimental setup and observations

An indoor test was done to acquire the yield as a component of evaporation and condensing cover temperatures in steady state. The distiller is demonstrated in Fig. 1. It comprises of steady temperature bath of 40 L volume with an evaporative surface area of 320 mm × 250 mm.

A transparent double-walled acrylic sheet of thickness 6 mm is used in side walls and single sheet is used in cover. An opening on the condensing chamber is provided

for distillate collection and it is placed above the constant temperature bath. Temperature of interior and exterior surface of cover, water and vapour temperature are determined by calibrated thermocouples.

Vapour is assumed at constant temperature throughout the still. Digital temperature indicator of least count of 0.1°C is used for representing temperature sensed by thermocouples. Heating coils are provided for heating water and stirrer is provided for maintaining uniform water temperature. An arrangement has been made at the top of condensing cover for placing the ice and drainage is provided to collect the melting ice. Measuring jar of accuracy 0.1 mL is provided for collecting the condensed water coming through pipe from the collecting trough. A gasket sealing is provided for preventing the vapour leakage from water bath.

Ice blocks are kept above the condensing cover to maintain its temperature closer to 0°C. Bore well water (TDS = 724 ppm) instead of brackish water is used in the experiments. There is no effect on the theoretical evaluation process by the use of this water as sea water (TDS = 30,000) vapour pressure is marginally less than fresh water vapour pressure (Murphy and Riley [34]). In experimentation, the observations (Table 1) are recorded by varying temperature of water from 35°C to 85°C in steps of 5°C and at a time difference of 10 min.

3. Assumptions

The following assumptions are implicit in the thermal analysis for the various components of the distiller (Fig. 1) viz. the flowing water film over the cover, the condensing cover, the basin water mass.

- The distiller operates in steady state.
- There is no temperature gradient across the condensing cover, that is, thermal resistance of the condensing cover is neglected.
- The temperature of inner surface of condensing cover and distillate is same.
- The temperature of water is uniform throughout.
- Area of condensing cover and basin area is same for inclination at 15°.
- Enclosure inside the still is considered to be non-absorbing and non-emitting.
- The condensing cover is opaque to the radiation coming from the water mass.

3.1. Energy balance for upward transfer of heat (numerical method)

3.1.1. For ice cooled condensing cover

The inside heat and mass transfer from surface of water to condensing surface occurs due to radiation ($\dot{q}_{rw}$), convection ($\dot{q}_{cw}$) and evaporation ($\dot{q}_{ew}$).

The energy balance equation between the water in basin area (A_b) and top of condensing cover (A_c) of the distiller in steady state is given as:

$$h_{1w}\left(T_w - T_c\right)A_b = h_{cf}\left(T_c - T_{wf}\right)A_c \tag{1}$$

(a)
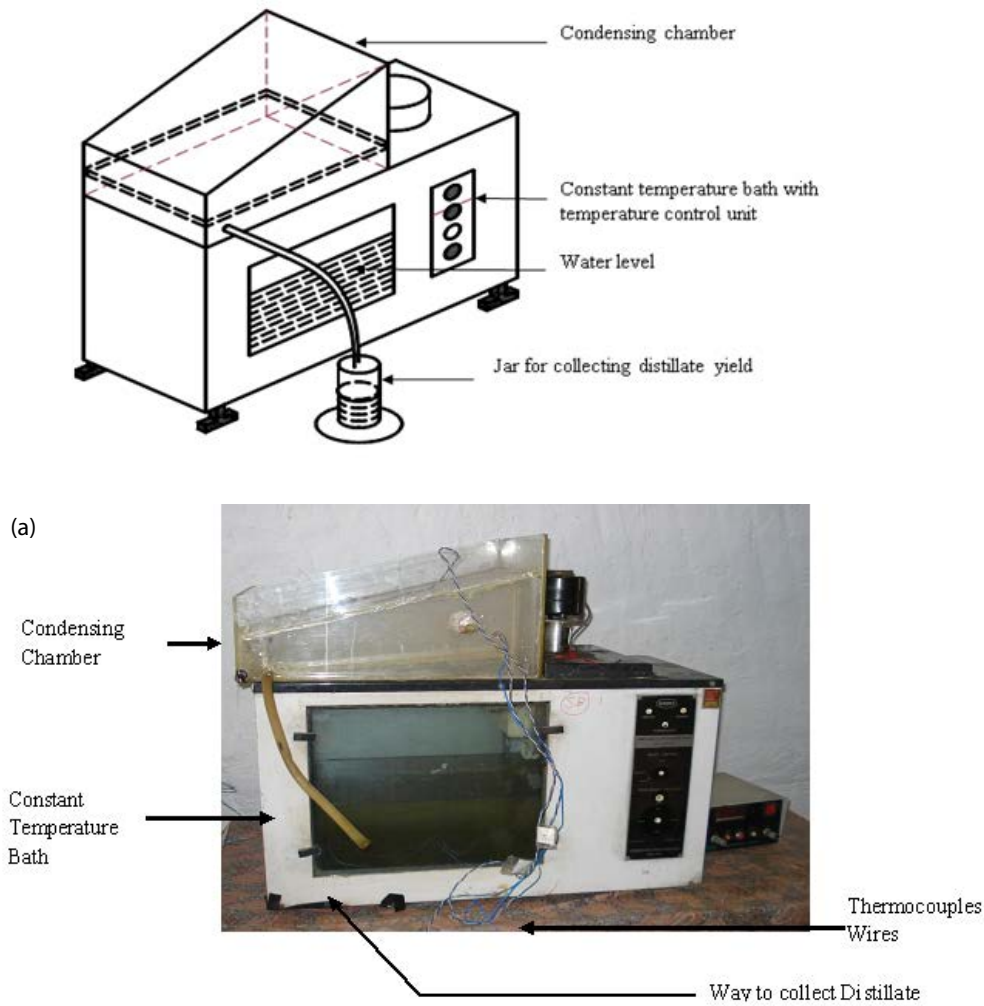
Fig. 1. Developed indoor distillation unit. (a) Line diagram of complete distillation system unit.

Heat balance for thin film of water mass flowing above the cover due to melting of ice can be given as:

$$h_{\mathrm{cf}}\left(T_c - T_{\mathrm{wf}}\right) = \dot{m}_i L + \dot{m}_{\mathrm{wf}} c_w dT_{\mathrm{wf}} + h_e\left(T_{\mathrm{wf}} - T_a\right) \tag{2}$$

where L = latent heat of fusion of ice and h_{cf} = convective heat transfer coefficient between cover and water film flowing over it.

The equivalent heat transfer coefficient (h_e) from water film to the ambient air is given by Singh and Tiwari [19]:

$$h_e = 0.016 h_w\left(\frac{P_{\mathrm{wf}} - \gamma P_a}{T_{\mathrm{wf}} - T_a}\right) + h_w; \qquad h_w = 2.8 + 3.0 V_a \tag{3}$$

The total upward inside heat transfer coefficient within the distiller is given by:

$$\dot{q}_{\mathrm{rw}} + \dot{q}_{\mathrm{cw}} + \dot{q}_{\mathrm{ew}} = h_{1w}\left(T_w - T_c\right) \times A_b \tag{4}$$

where h_{1w} is overall inside heat transfer coefficient and expressed as:

$$h_{1w} = h_{\mathrm{rw}} + h_{\mathrm{cw}} + h_{\mathrm{ew}} \tag{5}$$

The convective and evaporative heat transfer coefficients can be evaluated using Dunkle's [28] relation as follows:

$$h_{\mathrm{cw}} = 0.884\left[T_w - T_c + \frac{\left(P_w - P_c\right) \times \left(T_w + 273\right)}{268.9 \times 10^3 - P_w}\right]^{1/3} \tag{6}$$

$$h_{\mathrm{ew}} = 16.273 \times 10^{-3} \times h_{\mathrm{cw}}\left[\frac{P_w - P_c}{T_w - T_c}\right] \tag{7}$$

$$h_{\mathrm{rw}} = \in_{\mathrm{eff}} \sigma\left[\left(T_w + 273\right)^2 + \left(T_c + 273\right)^2\right]^2 \times \left(T_w + T_c + 546\right) \tag{8}$$

where $\in_{\mathrm{eff}} = \left[\dfrac{1}{\in_w} + \dfrac{1}{\in_c} - 1\right]^{-1} = 0.9$ between water and condensing surface.

3.1.2. For without cooled condensing cover

The energy balance equation between the water in basin area (A_b) and top of condensing cover (A_c) of the distiller exposed to ambient is given as:

$$h_{1w}\left(T_w - T_c\right)A_b = h_{2c}\left(T_c - T_{sky}\right)A_c \qquad (9)$$

In Eq. (9), the sink temperature is considered as sky temperature (T_{sky}) to get the more realistic values of h_{rcs}, rather than taking ambient temperature (T_a) as a sink temperature, especially under conditions that would exist during night time operation. The relation between sky temperature and ambient air is given by:

$$T_{sky} = 0.0552 \times T_a^{1.5} \qquad (10)$$

And,

$$h_{rcs} = \in_{eff} \sigma\left[\left(T_c + 273\right)^2 + \left(T_{sky} + 273\right)^2\right]^2 \times \left(T_c + T_{sky} + 546\right) \qquad (11)$$

Overall external heat transfer coefficient (h_{2c}) between cover and sky is given by:

$$h_{2c} = h_{rcs} + h_{ccs} = h_{rcs} + \frac{h_w\left(T_c - T_a\right)}{\left(T_c - T_{sky}\right)} \qquad (12)$$

Overall upward heat transfer coefficient is given by:

$$\frac{1}{h_o} = \frac{1}{h_{1w}} + \frac{1}{A_r \times h_{2c}} \qquad (13)$$

where $A_r = A_c / A_b$.

Internal heat transfer coefficients given by Eqs. (6)–(8) can be evaluated for the known values of water and cover temperatures. The value of partial pressure of water (P_w) and vapour (P_c) with change in temperature (10°C–90°C) is determined from the following expression [29]:

$$P(T) = \exp\left[25.317 - \frac{5144}{T}\right] \qquad (14)$$

where temperature, T, is in Kelvin and pressure is in Pascal.

3.2. Energy balance equations for two modes

3.2.1. For ice cooled condensing cover

Neglecting the absorption and heat capacity of cover, Eq. (1) can be rewritten by using Eqs. (2)–(8) as:

$$0.9\sigma\left[\left(T_w + 273\right)^4 - \left(T_c + 273\right)^4\right] +$$

$$0.884\left[T_w - T_c + \frac{\left(P_w - P_c\right) \times \left(T_w + 273\right)}{268.9 \times 10^3 - P_w}\right]^{1/3}\left(T_w - T_c\right)$$

$$+ 0.0163 h_{cw}\left(P_w - P_c\right) = A_r\left[h_{rcs} + \frac{h_w\left(T_c - T_a\right)}{\left(T_c - T_{sky}\right)}\right]\left(T_c - T_{sky}\right) \quad (15)$$

The non-linear energy balance Eq. (15) is resolved by approximate method for determining cover temperature (T_c) at particular water temperature (T_w). This is further used for finding heat transfer coefficients and distillate output numerically.

3.2.2. For without cooled cover

The non-linear energy balance Eq. (9) is resolved by approximate method for determining cover temperature (T_c) by using Eqs. (6)–(8) and (10)–(14) as:

$$0.9\sigma\left[\left(T_w + 273\right)^4 - \left(T_c + 273\right)^4\right] +$$

$$0.884\left[T_w - T_c + \frac{\left(P_w - P_c\right) \times \left(T_w + 273\right)}{268.9 \times 10^3 - P_w}\right]^{1/3}\left(T_w - T_c\right)$$

$$+ 0.0163 h_{cw}\left(P_w - P_c\right) = A_r\left[h_{rcs} + \frac{h_w\left(T_c - T_a\right)}{\left(T_c - T_{sky}\right)}\right]\left(T_c - T_{sky}\right) \quad (16)$$

3.3. Development of empirical relations to evaluate cover temperature

In order to achieve the result nearly close to numerical solution, non-linear relations for internal heat transfer coefficients and linear relations for external heat transfer coefficient have been developed.

The external heat transfer coefficients h_{cf} and h_{2c} are being developed in term of cover temperature. This is because of nearly constant indoor temperature during observation (15°C–20°C). On the basis of indoor experimental simulation, these expressions are developed for water temperature in range of 35°C–85°C. Further, this predicted value of cover temperature is used for determining heat transfer coefficients and yield.

3.3.1. For ice cooled cover

The following expressions are developed using experimental data during indoor simulation of the distiller operating with cooled cover with water temperature varying in range of 35°C–85°C.

$$h_{cw} = 1.54 + 0.024T_w + 1.91E - 6T_w^2 \qquad (17)$$

$$h_{ew} = 79.16 - 3.44T_w + 0.043T_w^2 \qquad (18)$$

$$h_{rw} = 4.69 + 0.0068T_w + 0.00046T_w^2 \qquad (19)$$

$$h_{1w} = 81.38 - 3.45T_w + 0.043T_w^2 \qquad (20)$$

$$h_{cf} = 21.89 + 0.32T_c \qquad (21)$$

The hourly distillate yield produced from distiller of 1 m² basin area is given as:

$$m_{ew} = 0.0894 - 0.0415T_w + 0.000725T_w^2 \qquad (22)$$

On solving Eq. (1) by using developed polynomials (Eqs. (20) and (21)), the quadratic equation obtained is as follows:

$$AT_c^2 + BT_c - C = 0 \qquad (23)$$

The solution for positive value of condensing surface temperature is written as:

$$T_c = \frac{-B + \sqrt{B^2 - (-4AC)}}{2A} \qquad (24)$$

where

$$A = 21.89 \qquad (25)$$

$$B = h_{1w} + 21.89 - 0.32T_{wf} = 103.27 - 3.45T_w + 0.043T_w^2 - 0.32T_{wf} \qquad (26)$$

$$C = h_{1w}T_w + 21.89T_{wf} = (81.38 - 3.45T_w + 0.043T_w^2)T_w + 21.89T_{wf} \qquad (27)$$

3.3.2. For without cooled cover

The following expressions are developed using experimental data reported by Tiwari and Tiwari [30] during indoor simulation of the distiller.

$$h_{cw} = 0.064T_w - 0.00029T_w^2 - 0.376 \qquad (28)$$

$$h_{ew} = 56.35 - 2.59T_w + 0.0345T_w^2 \qquad (29)$$

$$h_{rw} = 2.7 - 0.0038T_w + 0.000271T_w^2 \qquad (30)$$

$$h_{1w} = 58.68 - 2.46T_w + 0.03451T_w^2 \qquad (31)$$

$$h_{cf} = 5.42 + 0.031T_c \qquad (32)$$

The hourly distillate yield produced from distiller of 1 m² basin area is written as:

$$m_{ew} = 1.32 - 0.642T_w + 0.0084T_w^2 \qquad (33)$$

On solving Eq. (1) by using developed polynomials (Eqs. (31) and (32)), condensing surface temperature can be predicted similar to Eq. (24) using following parameters:

$$A = 5.42 \qquad (34)$$

$$B = h_{1w} + h_w + 5.42 - 0.031T_{sky} = 64.10 - 2.46T_w + 0.03451T_w^2 + h_w - 0.031T_{sky} \qquad (35)$$

$$C = h_{1w}T_w + h_wT_a + 5.42T_{sky} = \left(58.68 - 2.46T_w + 0.03451T_w^2\right)T_w + h_wT_a + 5.42T_{sky} \qquad (36)$$

Here, all the temperatures are in °C.

For particular water and condensing cover temperature, the distillate yield from the distiller of area A_b in time t can be estimated as:

$$m_{ew} = \frac{h_{ew}\left(T_w - T_c\right) \times A_b \times t}{h_{fg}} \qquad (37)$$

where h_{fg} is the latent heat of evaporation.

3.4. Methodology

Following procedure is being followed for development of the empirical relations:

- At particular water, condensing cover temperature and distillate yield, the convective, evaporative and radiative heat transfer coefficients have been calculated using Dunkle's relations.
- Assuming the non-linear equation for internal heat transfer coefficients (h_{cw}, h_{ew}, h_{rw} and h_{1w}), distillate yield and linear equation for the external heat transfer coefficient (h_c^2), that is,
- $h_{cw} = a + bT_w + cT_w^2$, $h_{ew} = a_1 + b_1T_w + c_1T_w^2$, and $h_{rw} = a_2 + b_2T_w + c_2T_w^2$
- $h_{1w} = a_1' + b_1'T_w + c_1'T_w^2$, $m_{ew} = a' + b'T_w + c'T_w^2$, and $h_{2c} = a_2' + b_2'T_w$
- The regressions analysis is used to determine the value of constants in equations of step 2 by using calculated heat transfer coefficient (as defined in step 1) and at particular water temperature.
- After finding constants of non-linear and linear equations (in step 3), the empirical relations of heat transfer coefficients and distillate yield are developed.
- The above said empirical relations are used to develop the empirical relation for the condensing cover temperature.
- At particular water temperature, empirical relations are used to determine cover temperature.
- Using particular water temperature and calculated value of cover temperature, the values of convective, evaporative, radiative heat transfer coefficients and fractional heat transfer have been calculated.

4. Results and discussions

Experimental measurements (Table 1) of indoor simulation are used for developing empirical relations (Eqs. (17)–(22)) for heat transfer coefficients. These expressions are solved for water temperature varying in range of 35°C–85°C, using digital computer technique. The heat transfer coefficients can be calculated at particular water temperature, water film temperature and ambient temperature, provided that the cover temperature is known to a reasonable accuracy.

Two approaches, numerical solutions of Eq. (15) and suggested equation Eq. (24) for ice and air cooled distiller is used to determine the cover temperatures and results are demonstrated in Fig. 2. Accuracy of the calculated value of cover temperature from suggested equations is ±1.0°C (maximum), exceptional at 30°C (±3.0°C) with variation of 3.6% from the values of numerical solution. The cover

Table 1
Measured temperature and yield for operating temperature range from 35°C–85°C

Set temperature of bath (°C)	Vapour temperature T_v (°C)	Water temperature T_w (°C)	Inner glass temperature T_c (°C)	Outer cover temperature T_{wf} (°C)	Yield in 10 min m_{ev} (kg)
35	27.3	36	20.2	3	0.0058
40	28.4	38.24	20.5	1.6	0.0068
45	31.5	42.5	23.6	1.1	0.0072
50	36.5	47.7	28.3	1.5	0.0100
55	40.4	53.4	34.2	0.1	0.0140
60	45.2	59.5	38.5	0.1	0.0180
65	53.2	66.7	43.2	1.2	0.0220
70	56.4	69.5	46.6	2.5	0.0270
75	62.7	75.5	55.3	2.7	0.0320
80	69.1	80.5	62.2	1.5	0.0380
85	75.1	86.5	69.6	3.4	0.0470
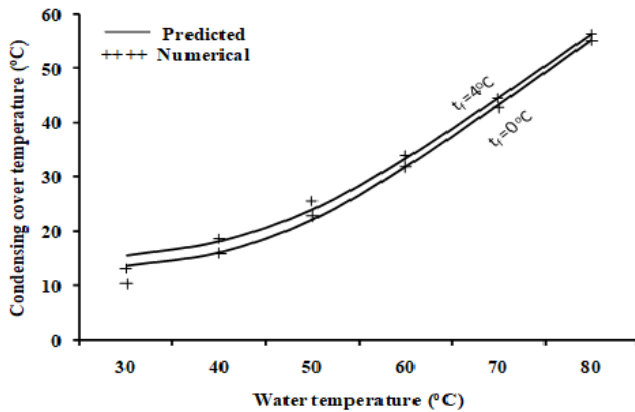
Fig. 2. Variation of condensing cover temperature with water temperature (ice cooled).

temperature decreases from 0.5°C to 0.2°C per degree decrease in water film temperature.

Cover temperature (T_c) calculated from numerical and suggested equations are further used for determining different heat transfer coefficients and this is demonstrated in Figs. 3a–c. The results obtained from the proposed Eq. (24) are compared with numerical solution of Eq. (15). The heat transfer coefficients are predicted precisely for varying range of water temperature and observed to be strongly correlated ($r = 0.99$).

In extreme condition, the maximum percentage deviation using proposed equations is 2%, 1.6% and 1% for convective, evaporative and radiative heat transfer coefficients respectively. Result shows that with rise in water film temperature, the convective heat transfer coefficient (h_{cw}) decreases, while there is marginal increase in evaporative and radiative heat transfer coefficients, which is less than 0.05 W/m²°C per degree rise in water film temperature for entire range. This has been also found that variation of evaporative heat transfer coefficient with water temperature is highly nonlinear due to exponential increase in vapour pressure. Overall heat balance of the solar still shows that h_{1w} is affected mostly by water temperature and comparatively

insensitive to water film temperature over the cover (shown in Fig. 3). This is due to decrease in film temperature, the glass covers temperature decreases, resulting increase in h_{cw} and marginal decrease in h_{ew} and h_{rw}.

The variation of outside convective heat transfer coefficient with cover temperature obtained using predicted and numerical value is shown in Fig. 4. The outside convective heat transfer coefficient (h_{cf}) varies linear with cover temperature and close agreement is observed with variation of ±0.5 W/m²°C (maximum) with the numerical solution, over entire ranges of other variables. It has verified that use of Eqs. (23)–(27) leads to negligible deviation in prediction of h_{cf} over the deviation in T_{wf} from 1°C to 4°C.

Fig. 5 demonstrates the comparative study of cover temperatures found by numerical solution of Eq. (16) and by suggested Eq. (24) with the help of expressions Eqs. (34)–(36) for distiller operating without cooled cover. The results expected are deviating by 2.0°C (maximum) from the T_c obtained using numerical solution and are in good agreement for entire range of variables h_w and T_w, and with maximum related deviation of 8.0%. As expected, with rise in wind heat transfer coefficient, the cover temperature decreases.

The computed values of cover temperature (T_c) found from numerical and suggested expressions are demonstrated in Figs. 6a–c. The observation shows that the calculated values of the heat transfer coefficients are predicted accurately for entire range of the variables. The maximum percentage deviation using proposed equations in convective, evaporative and radiative heat transfer coefficients are obtained as 5%, 1% and 1%, respectively, in extreme condition. It is observed that the convective heat transfer coefficient (h_{cw}) rises with rise in wind heat transfer coefficient, while evaporative heat transfer coefficients rise marginally.

At higher water temperature, there is significant effect of wind heat transfer coefficient. The computed values of external radiative heat transfer coefficient (h_{rcs}) are obtained less than internal radiative heat transfer coefficient (h_{rw}). The values decrease considerably with rise in wind heat transfer coefficient (h_w) due to decrement in glass cover temperature as depicted from Fig. 5. With rise in temperature of water, difference between inside and outside radiative heat transfer

(a)

(b)

(c)
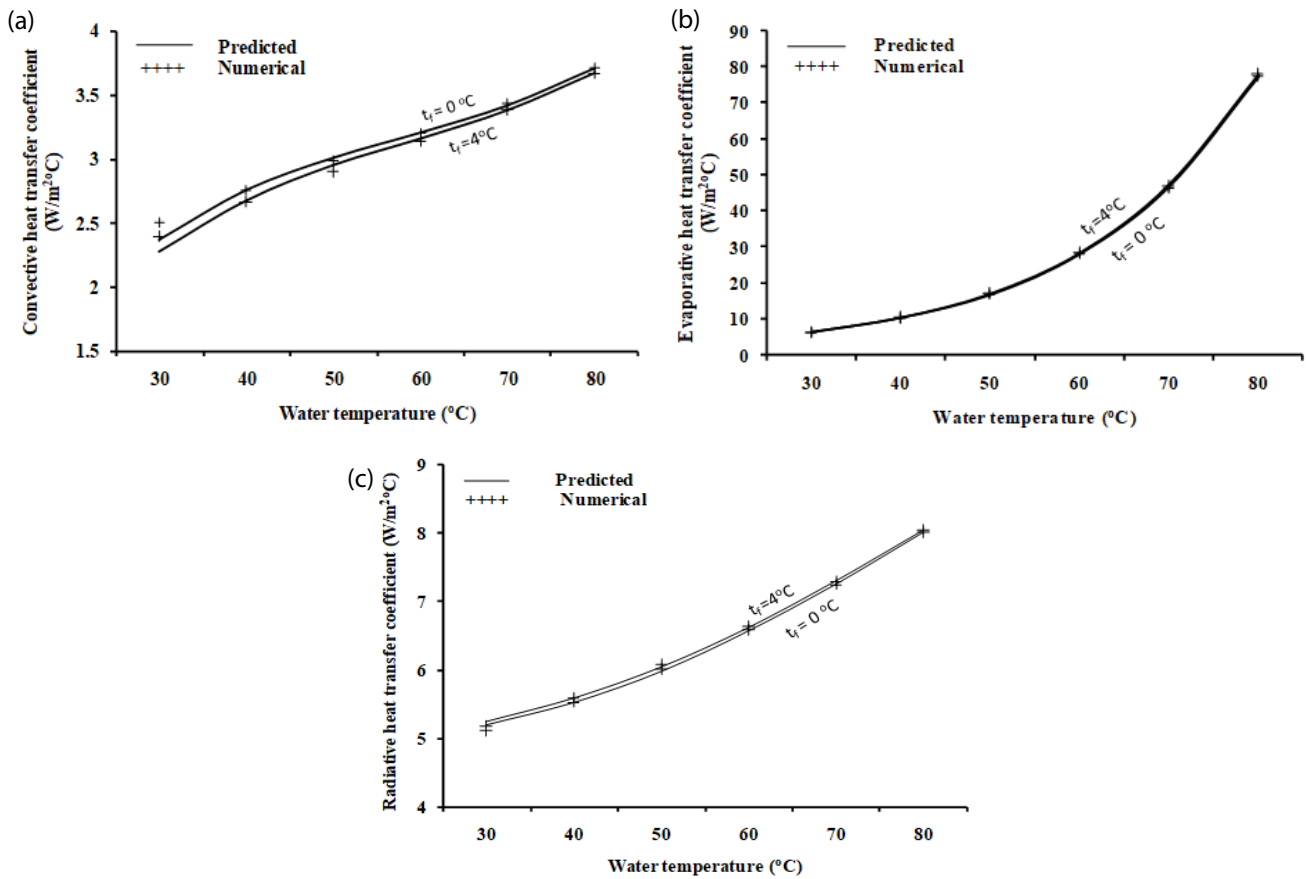
Fig. 3. (a) Variation of convective heat transfer coefficient with water temperature (ice cooled), (b) variation of evaporative heat transfer coefficient with water temperature (ice cooled) and (c) variation of radiative heat transfer coefficient with water temperature (ice cooled).
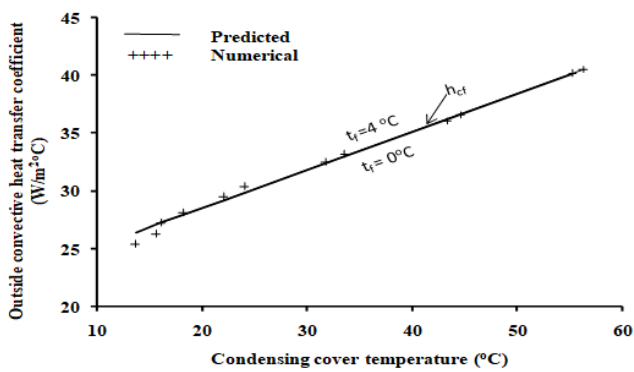
Fig. 4. Variation of outside convective heat transfer coefficient with condensing cover temperature (ice cooled).
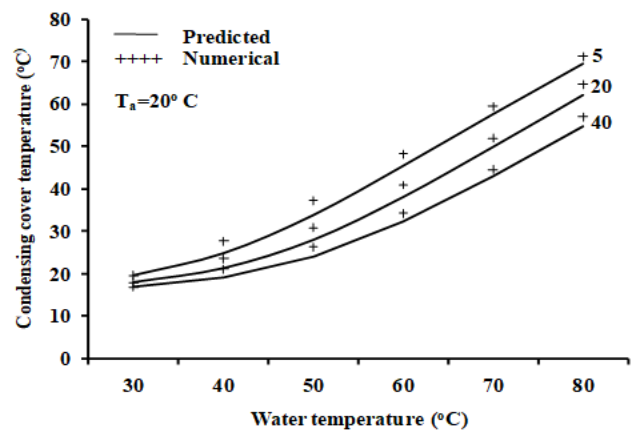
Fig. 5. Variation of condensing cover temperature with water temperature (without cooled).

coefficient diverges. It is observed that effect of wind heat transfer coefficient at lower water temperature (around 30°C) is insignificant, possibly due to low difference between glass and ambient temperature.

Fig. 7 shows the effect of ambient temperature (T_a) on condensing cover temperature for typical set of variables (T_w and h_w). With rise in water temperature, the effect is less significant with rise in ambient temperature. This is because at higher water temperatures, more water evaporated with

release of large amount of heat of condensation on inner surface. However, this released heat does not gets transferred to outer surface as rapidly as removal of heat from exterior surface because of thermal resistance of the cover material.

The expected values of condensing cover temperature (T_c) obtained from and numerical equations are validated
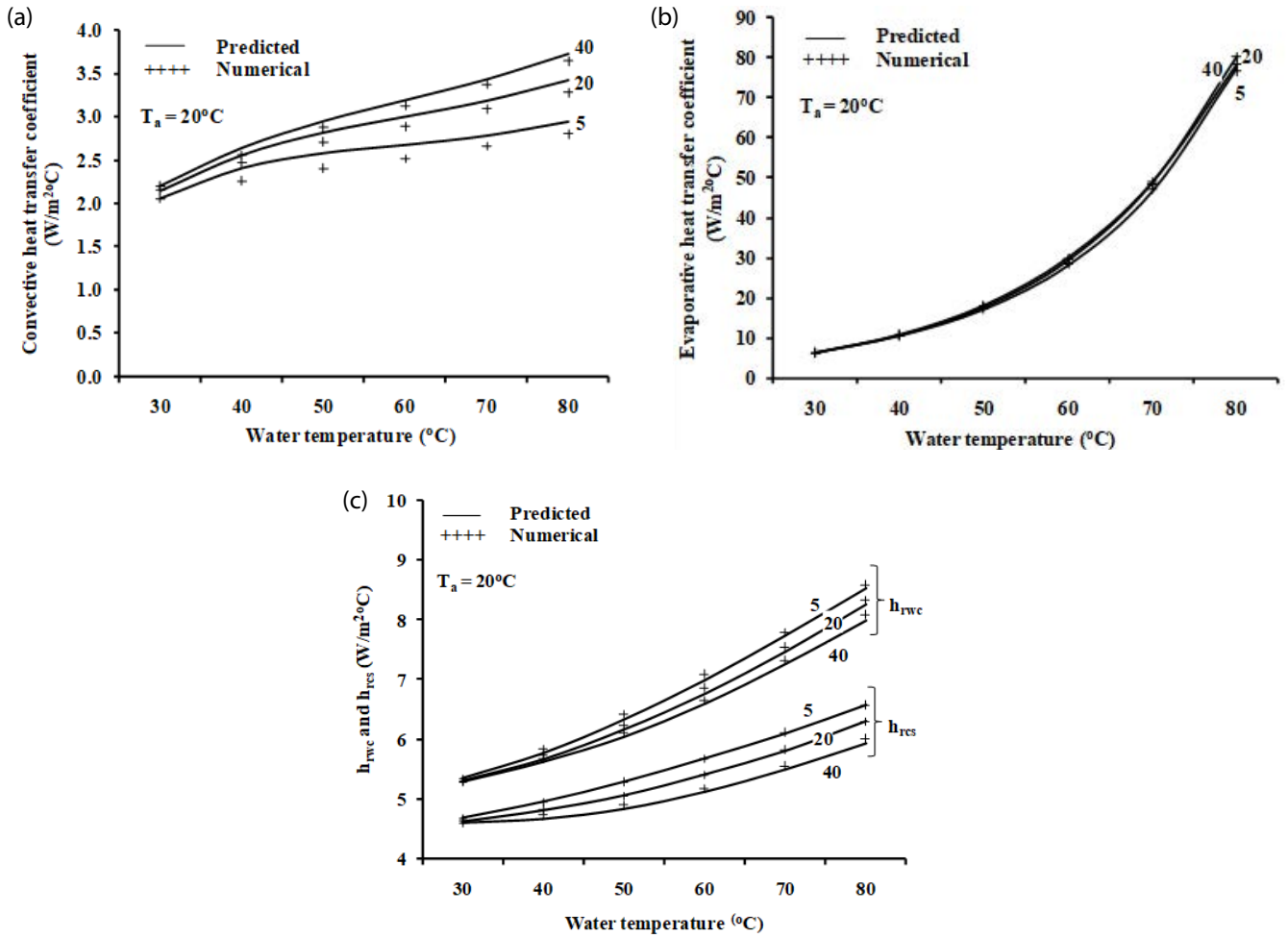
Fig. 6. (a) Variation of convective heat transfer with water temperature (without cooled cover), (b) variation of evaporative heat transfer with water temperature (without cooled cover), (c) variation of inner and outer radiative heat transfer with water temperature (without cooled cover).
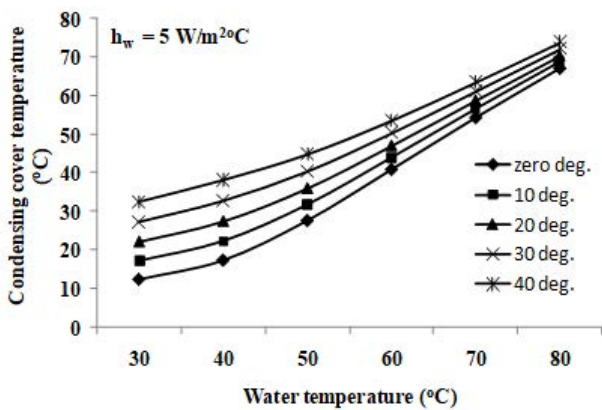
Fig. 7. Variation of condensing cover temperature with ambient air temperature (without cooled).

with experimental values of the distillate yield for the cooled cover distiller using Eq. (37). The results obtained are shown in Fig. 8. Experimental results deviate by 8% while numerical results by 3% from expected result obtained

from suggested condensing cover temperature (T_c) for full range of water temperature. Higher deviations (more than 20%) are observed at water temperature above 80°C. This is because of over expected values of convective and evaporative heat transfer coefficient at higher temperature due to limitation in Dunkle's model (50°C) and neglecting the thermal resistance/absorptivity of cover in the theoretical analysis. To reduce the deviation at higher water temperature (above 60°C), the corrective values of h_{1w} has been incorporated for developing the relation for the values of h_{1w} using Kumar and Tiwari model [31]. The empirical relation can be expressed as follows:

$$h_{1w} = 98.96 - 3.9T_w + 0.051T_w^2 \qquad (38)$$

It is proved that the corrected cover temperature (T_c) computed by using Eqs. (23)–(27) and h_{1w} from Eq. (38), deviates 9% in the temperature range above 60°C with experimental values. The yield expected from corrected temperature is nearer to the experimental results with maximum deviation of 5.7% obtained at 86°C temperature.

Table 2
Technical specification of the instruments used in the experiments

Instruments used	Accuracy	Range	Standard uncertainty
Constant temperature water bath	±0.5°C	–20°C to 400°C	0.288
Measuring jar	0.1 mL	0–5 mL	0.058
Stop watch	0.001 s	0–24 h	0.00058
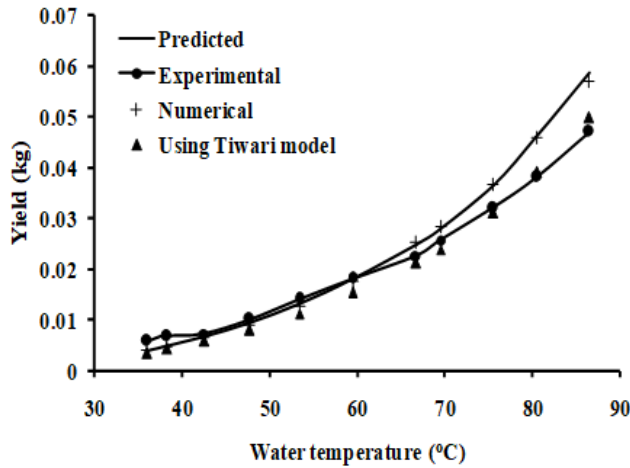
Fig. 8. Validation of predicted yield from numerical and experimental values for ice-cooled condensing cover.

4.1. Uncertainty analysis

Uncertainty is the key factor for determining the accuracy of the measured data. Uncertainty in the data is of two types, type A is due to random error and type B due to systematic error. The data are uniformly distributed, so here the type B uncertainty is calculated. The standard uncertainty of the instruments used for measurement is given by Eq. (39) [32,33]. The accuracy and standard uncertainty of the instruments used is shown in Table 2.

$$\text{Standard Uncertainty} = \frac{\text{Accuracy of instrument}}{\sqrt{3}} \quad (39)$$

5. Conclusions

The empirical equations are developed for finding the heat transfer coefficient, condensing cover temperature and distillate yield for the distiller operating in steady state for ice cooled and without cooled cover. The conclusion of the experimentation is given below:

- The proposed procedure simplifies computation of the internal heat transfer coefficients and cover temperature for distiller. The observed value and numerical values are closer to each other. The relative deviation is less than 2%. Internal heat transfer coefficients are predicted with percentage deviation less than 3.2% from the experiment.
- The percentage deviation occurs to determine the cover temperature for ice cooled and without cooled distiller are 3.6% and 8%, respectively, from the numerical. This

much accuracy is acceptable to calculate the heat transfer coefficients in different mode.
- The predicted yield has maximum relative variation of 3% from numerical and 5.7% from the experimental results after incorporating the suggested correction in the relation of overall internal heat transfer coefficient.

Symbols

A_b	–	Basin area of distiller, m²
A_c	–	Area of condensing cover, m²
A_r	–	Ratio of cover area to basin area
t	–	Small time interval, s
h_{cw}	–	Convective heat transfer coefficient between water and condensing cover, W/m²°C
h_{ew}	–	Evaporative heat transfer coefficient between water and condensing cover, W/m²°C
h_{rw}	–	Radiative heat transfer coefficient between water and condensing cover, W/m²°C
h_{1w}	–	Total internal heat transfer coefficient between water and condensing cover, W/m²°C
h_w	–	Wind heat transfer coefficient, W/m²°C
h_{cf}	–	Convective heat transfer coefficient between cover and flowing water film, W/m²°C
h_e	–	Equivalent heat transfer coefficient from water film to the ambient air, W/m²°C
h_o	–	Overall upward heat transfer coefficient, W/m²°C
h_{rcs}	–	Radiative heat transfer coefficient between cover and sky, W/m²°C
h_{ccs}	–	Convective heat transfer coefficient between cover and sky, W/m²°C
h_{2c}	–	Total upward heat transfer coefficient from cover to sky, W/m²°C
L	–	Latent heat of fusion, J/kg
m_{ew}	–	Distillate yield from distiller in time t, kg
P_a	–	Partial vapour pressure at ambient temperature, N/m²
P_c	–	Partial vapour pressure at inner surface temperature of cover, N/m²
P_w	–	Partial vapour pressure at water surface temperature, N/m²
P_{wf}	–	Partial vapour pressure at flowing water film temperature, N/m²
t	–	Time, s
T_a	–	Ambient temperature, °C
T_c	–	Condensing cover temperature, °C
T_{wf}	–	Water film temperature adjacent to condensing cover, °C
T_w	–	Water temperature in the basin, °C
dT_{wf}	–	Rise in water film temperature after melting of ice, °C

V_a	–	Wind velocity, m/s
$\dot{m}_i$	–	Melting rate of ice over the condensing cover, kg/s
$\dot{m}_{wf}$	–	Water flow rate over the condensing cover, kg/s
$\dot{q}_{cw}$	–	Rate of convective heat transfer, W/m²
$\dot{q}_{ew}$	–	Rate of evaporative heat transfer, W/m²

Greek

γ	–	Relative humidity
σ	–	Stefan–Boltzmann constant (5.6697×10^{-8} W/m²K⁴)
ε_g	–	Emissivity of glass
ε_w	–	Emissivity of water
ε_{eff}	–	Effective emissivity

References

[1] A. Cipollina, C. Sommariva, G. Micale, Efficiency increase in thermal desalination plants by matching thermal and solar distillation: theoretical analysis, Desalination, 183 (2005) 127–136.

[2] P.I. Cooper, Digital simulation of transient solar still processes, Sol. Energy, 12 (1969) 313–331.

[3] A.A. El-Sebaii, Effect of wind speed on active and passive solar stills, Energy Convers. Manage., 45 (1999) 1187–1204.

[4] M.A. Hamdan., A.M. Musa, B.A. Jubran, Performance of solar still under Jordan climatic conditions, Energy Convers. Manage., 40 (1999) 495–503.

[5] H.S. Aybar, H. Assefi, Simulation of a solar still to investigate water depth and glass angle, Desal. Wat. Treat., 7 (2009) 35–40.

[6] A.J.N. Khalifa, A.M. Hamood, Experimental validation and enhancement of some solar still performance correlations, Desal. Wat. Treat., 4 (2009) 311–315.

[7] O.O. Badran, H.A. Al-Tahaineh, The effect of coupling a flat-plate collector on the solar still productivity, Desalination, 183 (2005) 137–142.

[8] R. Tripathi, G.N. Tiwari, Thermal modeling of passive and active solar stills for different depths of water by using the concept of solar fraction, Sol. Energy, 80 (2006) 956–967.

[9] H. Al-Hinai, M.S. Al-Nassri, B.A. Jubran, Effect of climatic, design and operational parameters on the yield of a simple solar still, Energy Convers. Manage., 43 (2002) 1639–1650.

[10] M. Telkes, Improved Solar Stills' Transactions of the Conference on the Use of Solar Energy: The Scientific Basis, Tuscon Arizona, Vol. 3 1955, pp. 145–153, Chapter 14, Part 2.

[11] OG. George, Solar Distillation of Sea Water in the Virgin Islands, United State Department of Interior, Office of Saline Water, Research and Development Progress Report No. 5, 1955, pp. 1–39.

[12] G.O.G. Lof, J.A. Eibling, J.W. Bloemer, Energy balances in solar distillers, AIChE J., 7 (1961) 641–649.

[13] R.N. Morse, W.R.W. Read, A rational basis for the engineering development of a solar still, Sol. Energy, 12 (1968) 5–17.

[14] G.N. Tiwari, A. Minocha, P.B. Sharma, M. Emran Khan, Simulation of convective mass transfer in a solar distillation process, Energy Convers. Manage., 38 (1997) 761–770.

[15] G.N. Tiwari, Md. Emran Khan, R.K. Goyal, Experimental study of evaporation in distillation, Desalination, 115 (1998) 121–128.

[16] R.S. Adhikari, A. Kumar, A. Kumar, Estimation of mass-transfer rates in solar stills, Int. J. Energy Res., 14 (1990) 737–744.

[17] M.K. Phadatare, S.K. Verma, Effect of cover materials on heat and mass transfer coefficients in a plastic solar still, Desal. Wat. Treat., 2 (2009) 248–253.

[18] H.Z. Yousef, K.A.-A. Mousa, Modelling and performance analysis of a regenerative solar desalination unit, Appl. Therm. Eng., 24 (2004) 1061–1072.

[19] S.K. Singh, G.N. Tiwari, Analytical expression for thermal efficiency of a passive solar still, Energy Convers. Manage., 32 (1991) 571–576.

[20] W.N. Grune, R.A. Collins, R.B. Hughes, T.L. Thompson, Development of Improved Solar Still, United State Department of Interior, Office of Saline Water, Research and Development Progress Report No. 60, March 1962.

[21] B.W. Tleimat, E.D. Howe, Nocturnal production of solar distillers, Sol Energy, 10 (1966) 61–66.

[22] M.A.S. Malik, V.V. Tran, Final Report on Nocturnal Production of Petit St. Vincent Solar Still Using an Alternative Heat Source, Brace Research Institute of McGill University, T.20, 1969.

[23] M.A.S. Malik, V.M. Puri, H. Aburshaid, Use of double stage solar still for nocturnal production, Proceedings of 6th International Symposium on Fish Water from Sea, 2 (1978) 367.

[24] S.O. Onyegegbu, Nocturnal distillation in basin-type solar stills, Appl. Energy, 24 (1986) 29–42.

[25] V.B. Sharma, S.C. Mullick, Estimation of heat-transfer coefficients, the upward heat flow, and evaporation in a solar still, ASME, J. Sol. Energy Eng., 113 (1991) 36–41.

[26] S. Kumar, S. Sinha, Transient model and comparative study of concentrator coupled regenerative solar still in forced circulation mode, Energy Convers Manage., 37 (1996) 629–636.

[27] E. Sartori, Solar still versus solar evaporator: a comparative study between their thermal behaviors, Sol. Energy, 56 (1996) 199–206.

[28] R.V. Dunkle, Solar Water Distillation; The Roof Type Solar Still and a Multi Effect Diffusion Still, International Developments in Heat Transfer, ASME, Proceedings in International Heat Transfer, Part V, University of Colorado, 1661, p. 895.

[29] S. Kumar, G.N. Tiwari, Estimation of convective mass transfer in solar distillation systems, Sol. Energy, 57 (1996) 459–464.

[30] A.Kr. Tiwari, G.N. Tiwari, Effect of the condensing cover's slope on internal heat and mass transfer in distillation: an indoor simulation, Desalination, 180 (2005) 73–78.

[31] S. Kumar, G.N. Tiwari, Estimation of internal heat transfer coefficients of a hybrid (PV/T) active solar Still, Sol. Energy, 83 (2009) 1656–1667.

[32] N. Rahbara, A. Asadi, E. Fotouhi-Bafghi, Performance evaluation of two solar stills of different geometries: tubular versus triangular: experimental study, numerical simulation, and second law analysis, Desalination, 443 (2018) 44–55.

[33] S. Nazari, H. Safarzadeh, M. Bahiraei, Performance improvement of a single slope solar still by employing thermoelectric cooling channel and copper oxide nanofluid: an experimental study, J. Cleaner Prod., 208 (2019) 1041–1052.

[34] J. Murphy, J.P. Riley, The storage of sea-water samples for the determination of dissolved inorganic phosphate, Anal. Chim. Acta, 14 (1956) 318–319.